ARTICLE

Vol. 12, No. 1, 2021
ISSN 2233-4203/ e-ISSN 2093-8950
www.msletters.org | Mass Spectrometry Letters

Boron Detection Technique in Silicon Thin Film Using Dynamic Time of Flight Secondary Ion Mass Spectrometry

M. Abul Hossion[1]* and Brij M. Arora[2]

[1]*Department of Physics, BSMR Maritime University, Dhaka 1216, Bangladesh*
[2]*Department of Physics, University of Mumbai, Mumbai 400098 India*

Received March 5, 2021, Revised March 25, 2021, Accepted March 25, 2021
First published on the web March 31, 2021; DOI: 10.5478/MSL.2021.12.1.26

Abstract : The impurity concentration is a crucial parameter for semiconductor thin films. Evaluating the impurity distribution in silicon thin film is another challenge. In this study, we have investigated the doping concentration of boron in silicon thin film using time of flight secondary ion mass spectrometry in dynamic mode of operation. Boron doped silicon film was grown on i) p-type silicon wafer and ii) borosilicate glass using hot wire chemical vapor deposition technique for possible applications in optoelectronic devices. Using well-tuned SIMS measurement recipe, we have detected the boron counts 10^1~10^4 along with the silicon matrix element. The secondary ion beam sputtering area, sputtering duration and mass analyser analysing duration were used as key variables for the tuning of the recipe. The quantitative analysis of counts to concentration conversion was done following standard relative sensitivity factor. The concentration of boron in silicon was determined 10^{17}~10^{21} atoms/cm^3. The technique will be useful for evaluating distributions of various dopants (arsenic, phosphorous, bismuth etc.) in silicon thin film efficiently.

Keywords : ToF-SIMS, HWCVD, boron concentration, p-type silicon, RSF, thin film.

Introduction

Secondary ion mass spectrometry is an established method for identification and quantification of isotopes and elements on the top surface or below the surface of a solid sample. Dopant concentrations and their depth distribution are of major importance for the electrical performance of semiconductor devices such as transistors and optoelectronic devices such as sensors, photovoltaic devices etc. Due to the high detection sensitivity, secondary ion mass spectrometry (SIMS) is widely used for the determination of impurity concentration of dopant materials in silicon thin films.[1] Since its inception in 1949, the major improvement in instrumentation came in 1980-2013.[2] Depending on the mass analyser, available types of instrumentation of SIMS are i) Magnetic sector ii) Quadruple and iii) Time of Flight (ToF).[3,4] The data acquisition of SIMS is performed in two distinct modes of operation, the static and dynamic modes. In the static mode, materials from several points of the top surface of a sample is sputtered. In the dynamic mode, materials from a single point on the top surface of a sample is sputtered to produce a crater which provides in-depth data of elements.[5] The mass spectrum is obtained by rastering the top of the sample surface using a pulsed primary ion gun followed by sputtering the region using secondary ion gun.[6]

The detection, interpretation and identification of the isotope of interest is crucial as the detector detects a cluster of different isotopes.[7,8] The process becomes further challenging for thin film devices such as transistors, sensors and photovoltaic devices, where the distribution of dopants dictates the performance of the device.[9-11] An established method for the data analysis is to use a reference sample of known impurity concentration obtained from ion implantation techniques.[12] The availability of the ion implantation facility and reference samples limits the characterization process.

In this article, we demonstrate, how by using well-tuned conditions, the detection of Boron (B) in silicon thin film can be performed by time of flight secondary ion mass spectrometry (ToF-SIMS) using dynamic mode of operation efficiently. In most works using SIMS measurement, only the final results are tabulated. In this work, primary ion beam raster area, secondary ion beam sputtering area, sputtering duration and mass analyser

Open Access

*Reprint requests to M. Abul Hossion, orcid.org/0000-0002-3199-1682
E-mail: abulhossion.phy@bsmrmu.edu.bd

All MS Letters content is Open Access, meaning it is accessible online to everyone, without fee and authors' permission. All MS Letters content is published and distributed under the terms of the Creative Commons Attribution License (http://creativecommons.org /licenses/by/3.0/). Under this license, authors reserve the copyright for their content; however, they permit anyone to unrestrictedly use, distribute, and reproduce the content in any medium as far as the original authors and source are cited. For any reuse, redistribution, or reproduction of a work, users must clarify the license terms under which the work was produced.

analysing duration were used as key variables for well-tuned recipe are specified. The data acquisition and interpretation were followed by conversion of counts to concentration using relative sensitivity factor (RSF) procedure.

Experimental

Sample preparation

Samples used in this work were thin films synthesized by hot wire chemical vapor deposition (HWCVD) technique, widely used because of its simplicity of operation. Initially, thin ~20 nm nucleation layer of intrinsic silicon was grown on i) p-type silicon (100) single side polished wafer (89-Boron) and ii) alkali free borosilicate corning 7059 glass (88-Boron), as substrate, at 400°C with a gas ratio SiH_4:H_2 = 1:20 for 100 s. Filament temperature was kept at 1900°C at all stages. After the nucleation stage, a mixture of silane (SiH_4) and hydrogen (H_2) were used as process gas with a ratio of SiH_4:H_2 = 5:15 for 20 min at 600°C substrate temperature. The intrinsic silicon film was annealed at this stage under 20 sccm (standard cubic centimetre per minute) of H_2 flow for 30 min followed by a H_2 soaking, during cooling the sample from the growth temperature to a lower temperature of 200°C for another 45 min.[13] These poly crystalline intrinsic silicon films have (220) preferred crystalline orientation.[14] At this stage boron containing gas (5% diborane in hydrogen) was introduced with a gas ratio SiH_4:5%B_2H_6:H_2 = 1:1:20 for 10 min to grow the amorphous boron doped layer. The thicknesses of intrinsic silicon film and boron doped film are 800 nm and 100 nm respectively, estimated from cross sectional transmission electron microscopy.[15] A boron diffused silicon wafer was used as reference to validate the data acquisition technique and comparison of boron concentration of this study to values shown in other literature.[16-18] The reference boron diffused sample was prepared using standard diffusion furnace at 1000°C for 20 min on 2 inch diameter p-type silicon wafer. This diffusion process allowed the boron atoms to diffuse into the Si wafer to a depth of about 1000 nm.

Depth profile analysis

The total crater depth was measured using Veeco Dektak 150 surface profiler and the data given in Figure 1 and Table 1. The sputtering rate was obtained from the total crater depth divided by the total sputtering duration. The sputtering rate for reference boron diffused silicon wafer is 0.34 nm/s, where the crater depth is 1416 nm as shown in Figure 1(i) and total sputtering duration is 4120 s. The sputtering rate for 89-Boron doped intrinsic silicon thin film using HWCVD is 0.39 nm/s, where the total crater depth is 1266 nm as shown in Figure 1(ii) and total sputtering duration is 3260 s. The duration of mass analyser analysing duration was deducted from the total time to calculate actual sputtering duration.

TOF-SIMS data acquisition

The detection of secondary ions is carried out using a mass analyser based on the time of flight principle: ions are accelerated into a flight tube and measures the exact flight duration. Thus, ions are separated by the time of flight analysis from which a mass spectrum is generated.[19,20]

To measure the secondary ion counts, the PHI nano TOF II TRIFT was used from Physical Electronics, MN, USA. In this process, a 10 ns pulsed liquid metal ion gun (LMIG) uses Gallium sources to produce (Ga^+) ions as primary ion

Table 1. Veeco Dektak 150 surface profiler data for the crater depth and the scanning length.

Sample Name	Cursor Position	Cursor Width (mm)	X-axis position (mm)	Crater Length (mm)	Y-axis position (nm)	Crater Depth (nm)
Reference boron	Left	0.1668	0.9212	1.2574	111.32	1416.74
	Middle	0.2113	1.5499		-1381.18	
89-Boron	Left	0.1668	0.2285	1.6328	42.1655	1266.16
	Middle	0.2039	1.0449		-1242.14	

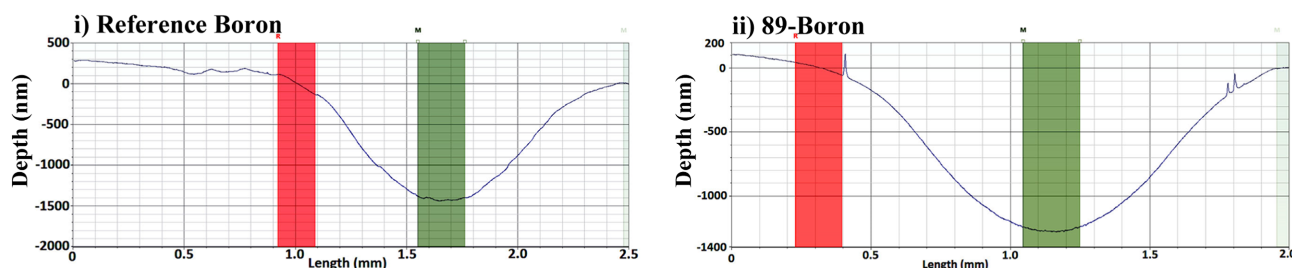

Figure 1. The surface profile of the total depth of the crater for i) reference boron diffused silicon wafer is 1416 nm and ii) 89-Boron doped intrinsic silicon thin film using HWCVD is 1266 nm measured using Veeco Dektak 150 surface profiler.

Table 2. ToF-SIMS scanning parameters for the detection of boron isotope (^{11}B) and silicon isotope (^{30}Si) in silicon thin film using oxygen ion (O^{2+}) sputtering gun.

Sample Name	Boron thin film thickness (nm)	Sputtering beam current (A)	Sputtering beam Energy (kV)	Sputtering beam raster area (μm^2)	Sputtering duration (s)	Mass analyser analysing duration (s)
Reference boron	1000	8.4×10^{-7}	3	200 × 200	20	60
89-Boron	100			400 × 400		

Table 3. Part of data for the conversion of ToF-SIMS data to concentration-depth profile. The complete data set is provided as supporting information.

Cycle number (A)	Sputtering Duration (s) (B)	Total Time (s) (A×B)	Sputtering rate (nm/s) (C)	Crater depth (nm) [(A×B)C]	Measured Intensity of ^{11}B isotope (counts)	Measured Intensity of ^{30}Si isotope (counts)	Boron concentration (atoms/cm^3)
i) Reference Boron diffused silicon wafer							
1	20	20	0.34	6.88	4333	113765	8.26E+19
2	20	40	0.34	13.75	8470	138927	1.32E+20
3	20	60	0.34	20.63	11015	140310	*1.70E+20
ii) 89-Boron doped intrinsic silicon thin film using HWCVD							
1	20	20	0.39	7.77	50365	33616	3.25E+21
2	20	40	0.39	15.53	58367	46138	2.75E+21
3	20	60	0.39	23.30	56577	47072	2.61E+21

*Using equation-1, $C_B = 7\times10^{22}\times0.031\times(\frac{11015}{140310}) = 1.720\times10^{20}$ atoms/cm^3

beam to ionise the surface molecules.[21] The beam energy was kept 30 kV with a beam current of 8×10^{-9} A and the raster size 200 × 200 μm^2.[22] The oxygen ion (O^{2+}) gun was used as sputtering tool to produce positive secondary ions.[23]

In this study, the boron isotope (^{11}B) and silicon isotope (^{30}Si) were detected. The scanning parameters are given in Table 2. For sample with lower impurity concentration, the ion counts can be increased by allowing the mass analyser to analyse for longer duration. The tuning was also performed on the sputtering area. For thinner sample, a larger sputtering area was used where, for thicker sample, a smaller sputtering area allows the sputtering to occur deeper. The sputtering beam raster area given in the Table 2 was selected by performing the sputtering at different locations on the sample with the variation of the raster size range 100 × 100 μm^2 to 600 × 600 μm^2.

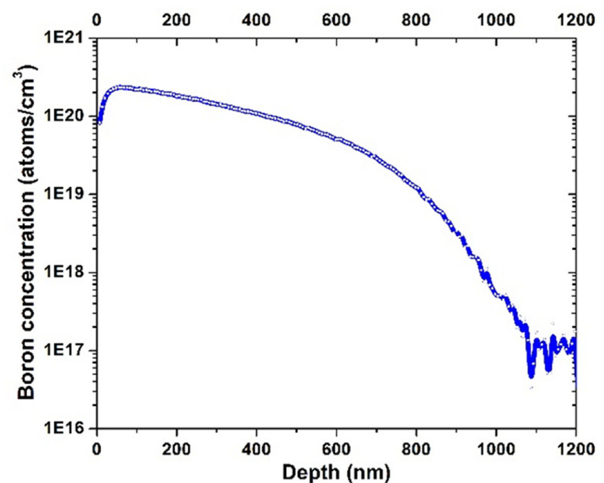

Figure 2. Boron concentration – depth curve of Reference boron diffused silicon wafer

Results and Discussion

The ToF-SIMS signal is interpreted using relative sensitivity factor for Boron Counts to concentration conversion. The concentration of boron (C_B) in silicon is calculated using the following equation 1,

$$C_B = RSF_{B(Si)} \times \%^{30}Si \times (\frac{I_{B(Si)}}{I_{30Si}}) \quad (1)$$

Here, C_B is Concentration of boron in silicon, $RSF_{B(Si)}$ is relative sensitivity factor of boron in silicon,[6] $\%^{30}Si$ is fractional isotope abundance of ^{30}Si in silicon,[24] $I_{B(Si)}$ is intensity of boron isotope (^{11}B) counts and I_{30Si} is intensity of silicon isotope (^{30}Si) counts with oxygen (O^{2+}) gun using ToF-SIMS. Table 3 shows the part of data used in the Boron counts to concentration conversion calculation. The complete data table is provided with the article as supporting information.

 ©Korean Society for Mass Spectrometry

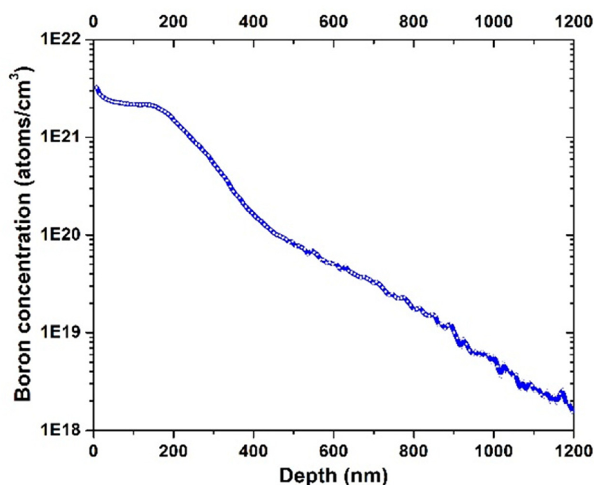

Figure 3. Boron concentration – depth curve of 89-Boron doped intrinsic silicon thin film using HWCVD.

Table 3 is used to plot Boron concentration versus crater depth curve for i) Reference Boron and ii) 89-Boron as shown in Figure 2 and 3 respectively. Figure 2 shows the concentration of boron, diffused in p-type silicon wafer for Reference Boron sample. The concentration at the top surface of the wafer is 2×10^{20} atoms/cm^3 which decreases with the depth. Figure 3 shows the concentration of boron in intrinsic silicon thin film grown using HWCVD. The concentration is 3.25×10^{21} atoms/cm^3 at the top amorphous layer. This remain uniform over the top 150 nm and then starts to decrease as it reaches the lower intrinsic silicon thin film. This shows that the intrinsic silicon film also gets diffused by boron atoms. This may happen due to the reason that the out-diffusion of boron atoms from the wafer at high (600°C substrate and 1900°C filament) process temperature contaminated the intrinsic silicon film.[25-27] The Boron concentration in the reference boron diffused silicon wafer shown in Figure 2 is 1×10^{20} atoms/cm^3 at 400 nm which is in close agreement with the data found in other measurements.[28-30] At room temperature the boron concentration in 200 μm silicon wafer published in other literature was found 7×10^{20} atoms/cm^3 using hot probe method.[31]

Conclusions

The concentration of boron in silicon thin film was measured using versatile ToF-SIMS technique. Relative sensitivity factor was used to interpret the ToF-SIMS data of boron isotope and silicon matrix element. The boron in silicon detected on the top surface of amorphous boron doped silicon thin film was 3.25×10^{21} atoms/cm^3 where 1×10^{18} atoms/cm^3 was detected at one-micron depth. The tuning of i) sputtering area to the thickness of thin film and ii) mass analyser analysing duration to the boron counts, provides an efficient route for the detection of dopants in the silicon thin film. The results of this study will be useful for the detection and quantification of impurities in wide area of thin films using complex ToF-SIMS technique.

Supporting Information

Supporting information is available at https://drive.google.com/file/d/1ME73GRSTLKC--v8qPjm68lpIePQtW4Dd/view?usp=sharing.

Acknowledgements

The authors thank Yuriy Kudriavtsev, Center for Research and Advanced Studies of the National Polytechnic Institute, Apodaca, Mexico, for the suggestions in data interpretation. The authors also thank to Dr. C. S. Harendranath, Principle research scientist, Sophisticated analytical instrument facility (SAIF), Indian Institute of Technology Bombay, Mumbai, India, for providing necessary laboratory facilities. The authors are grateful to Mr. Subhash Lokhre and Mr. Nilesh Marle for their active participation during measurement process. We are also grateful to HWCVD system team Anjum A., Poonam K., and Raorane, Centre of Excellence in Nanoelectronics (CEN), Indian Institute of Technology Bombay, Mumbai, India.

Author contributions

Both the authors Abul Hossion (A.H) and Brij Mohan Arora (B.M.A) participated in the conceptualization, designing methodology, analysis, interpretation, discussion and improvement of the manuscript of the experimental data on ToF-SIMS study on boron doped silicon film. A.H. collected and analysed the data followed by the manuscript preparation while B.M.A does the review, editing, supervision and funding acquisition. All the figures and images are prepared by A.H. Both the authors have read and agreed to the published version of the manuscript.

Funding

This research was funded by Centre of Excellence in Nano electronics (CEN) of the Indian Institute of Technology, Bombay, Mumbai, India.

Conflicts of interest

The authors declare no conflict of interest. The funders had no role in the design of the study; in the collection, analysis, or interpretation of data; in the writing of the manuscript, or in the decision to publish the results.

References

1. van der Heide, P. *Secondary Ion Mass Spectrometry: An Introduction to Principles and Practices 1st ed.*, Wiley & Sons: New York, **2014**.
2. Hofmann, J. P.; Rohnke, M.; Weckhuysen, B. M.; *Phys. Chem. Chem. Phys.* **2014**, 16, 5465, DOI: 10.1039/C3CP54337D.
3. Riviere, J. C.; Myhra, S.; Myhra, S. *Handbook of Surface and Interface Analysis: Methods for Problem-Solving 2nd ed.,* CRC Press, New York, **2009**, https://doi.org/10.1201/9781420007800.
4. Wilson, R. G. *Secondary ion mass spectrometry: a practical handbook for depth profiling and bulk impurity analysis.* Wiley & Sons: New York, **1989**.
5. Benninghoven, A.; Rudenauer, F. G.; Werner, H.W. *Secondary Ion Mass Spectrometry: Basic Concepts, Instrumental Aspects, Applications and Trends*, Wiley & Sons: New York, **1987**.
6. Stevie, F. *Secondary Ion Mass Spectrometry: Applications for Depth Profiling and Surface Characterization.* Momentum Press, New York, **2015**.
7. Priebe, A.; Xie, T.; Bürki, G.; Pethö, L.; Michler, J. J. *Anal. At. Spectrom*. **2020**, 35, 1156, DOI: 10.1039/C9JA00428A.
8. Collin, M.; Gin, S.; Jollivet, P.; Dupuy, L.; Dauvois, V.; Duffours, L.; *NPJ Mater. Degrad*. **2019**, 3, 1, DOI: 10.1038/s41529-019-0076-3.
9. Sandow, C.; Knoch, J.; Urban, C.; Zhao, Q.-T.; Mantl, S. *Solid State Electron*. **2009**, 53, 1126, DOI: 10.1016/j.sse.2009.05.009.
10. Kim, E.-Y.; Kim, J. *Adv. Mater. Sci. Eng.* **2013**, 2013, e974507. DOI: 10.1155/2013/974507.
11. Fang, W.; Ni, Z.; Wang, P.; Xiang, C.; Sun, T.; Zhang, J.; Wang, R.; Yang, J.; Yang, Y. *J. Mater. Sci: Mater. Electron.* **2020**, 31, 6398, DOI: 10.1007/s10854-020-03196-y.
12. Eswara, S.; Pshenova, A.; Lentzen, E.; Nogay, G.; Lehmann, M.; Ingenito, A.; Jeangros, Q.; Haug, F.-J.; Valle, N.; Philipp, P.; Hessler-Wyser, A.; Wirtz, T. *MRS Commun.* **2019**, 9, 916, DOI: 10.1557/mrc.2019.89.
13. Kaur, G.; Hossion, M. A.; Kulasekaran M; Arora, B. M. *IEEE 40th Photovoltaic Specialist Conference (PVSC)* **2014,** 1326, DOI: 10.1109/PVSC.2014.6925162.
14. Hossion, M. A., Arora, B. M. *IEEE 40th Photovoltaic Specialist Conference (PVSC)* **2014,** 1292, DOI: 10.1109/PVSC.2014.6925153.
15. Hossion, M. A.; Arora, B. M. *Int. J. Thin Film Sci. Tech.* **2020**, 9, 37, DOI: 10.18576/ijtfst/090106.
16. Fu, J.; Chen, K.; Chang, S.; Zhi, K.; Gao, X.; Wei, H.; Dan, Y. *AIP Adv.* **2019**, 9, 125219, DOI: 10.1063/1.5134118.
17. Dutta, S.; Pandey, A.; Saxena, G.; Raman, R.; Dhaul, A.; Pal, R.; Chatterjee, R. *J. Mater. Sci.: Mater. Electron.* **2012**, 23, 1569, DOI: 10.1007/s10854-012-0630-z.
18. Mirabella, S.; De Salvador, D.; Napolitani, E.; Bruno, E.; Priolo, F. *J. Appl. Phys.* **2013,** 113, 031101. https://doi.org/10.1063/1.4763353
19. Guilhaus, M. *J. Mass Spectrom.* **1995**, 30, 1519, DOI: 10.1002/jms.1190301102
20. Douglas, M. A.; Chen, P. J.; *Surf. Interface Anal*. **1998**, 26, 984, DOI: 10.1002/(SICI)1096-9918(199812)26:13<984::AID-SIA446>3.0.CO;2-K.
21. Bayly, A. R.; Waugh, A. R.; Anderson, K. *Nucl. Instrum. Methods Phys. Res*. **1983**, 218, 375, DOI: 10.1016/0167-5087(83)91009-8.
22. Kia, A. M.; Haufe, N.; Esmaeili, S.; Mart, C.; Utriainen, M.; Puurunen, R. L.; Weinreich, W. *Nanomaterials* **2019,** 9, 1035, DOI: 10.3390/nano9071035.
23. Beljakowa, S.; Pichler, P.; Kalkofen, B.; Hübner, R. *Phys. Status solidi A* **2019**, 216, 1900306, DOI: 10.1002/pssa.201900306.
24. Meija, J.; Coplen, T. B.; Berglund, M.; Brand, W. B.; De Bièvre, P.; Gröning, M.; Holden, N. E.; Irrgeher, J.; Loss, R. D.; Walczyk, T.; Prohaska, T. *Pure Appl. Chem.* **2016**, 88, 3, 265, DOI: 10.1515/pac-2015-0305.
25. Kurachi, I.; Yoshioka, K. *Int. J. Photoenergy* **2016**, 8183673, DOI: 10.1155/2016/8183673.
26. Perova, T. S.; Nolan-Jones, M.; McGilp, J.; Gamble, H. S. *J. Mater. Sci.: Mater. Electron.* **2016,** 27, 6292, DOI: 10.1007/s10854-016-4561-y.
27. Lill, P. C.; Dahlinger, M.; Köhler, J. R. *Materials* **2017**, 10, 189, DOI: 10.3390/ma10020189.
28. Park, C. J.; Kim, K. J.; Cha, M. J.; Lee, D. S. *Analyst* **2000**, 125, 493, DOI: 10.1039/A909215C.
29. Cojocaru-Mirédin, O.; Cadel, E.; Deconihout, B.; Mangelinck, D.; Blavette, D. *Ultramicroscopy* **2009**, 109, 649, DOI: 10.1016/j.ultramic.2008.09.008.
30. Pisonero, J.; Lobo, L.; Bordel, N.; Tempez, A.; Bensaoula, A.; Badi, N.; Sanz-Medel, A. *Sol. Energy Mater. Sol. Cells* **2010**, 94, 1352, DOI: 10.1016/j.solmat.2010.04.002.
31. Akter, N.; Afrin, S.; Hossion, A.; Kabir, K.; Akter, S.; Mahmood, Z. *Int. J. Adv. Mater. Sci. Eng.* **2015**, 4, 13, DOI: 10.14810/ijamse.2015.4402.

 ©Korean Society for Mass Spectrometry